

# Non-equilibrium Phase Transitions in a Cellular Signaling Chain

Supriya Krishnamurthy<sup>(1,2)</sup>, Eric Smith<sup>(1)</sup>, David Krakauer<sup>(1)</sup> and Walter Fontana<sup>(1)</sup>

(1): Santa Fe Institute, 1399 Hyde Park Road, Santa Fe, NM 87501, USA

(2): Laboratory of Physics, Helsinki University of Technology, HUT-02015, Finland

(Dated: December 23, 2018)

We construct and analyze a stochastic model of a signal-transduction chain, which consists of  $J+1$  sites representing the addition of phosphate groups on a set of  $N$  identical protein molecules. The protein molecules hop forward (a phosphorylation reaction) or backward (dephosphorylation) on this one-dimensional  $J+1$ -site lattice. Fully dephosphorylated (phosphorylated) proteins feed back to act as catalysts for all intermediate dephosphorylation (phosphorylation) reactions. This model exhibits a continuous phase transition at *any*  $J \geq 2$ , between a symmetric and a symmetry-breaking state. In addition, we find that the universality class of the phase transition at finite  $J$  is different than that at  $J \rightarrow \infty$ .

Molecular switches are a key component of many signal transduction and gene expression circuits that control cellular behavior such as the cell cycle [1, 2], differentiation [3, 4] and memory [5]. One sense of switching is termed ultrasensitivity, in which the character of a given steady state changes significantly within a small signal range [6]. A different mechanism associated with the establishment of “checkpoints” is bistable switching, the capacity of a circuit to flip between two stable states in response to an incoming signal [7].

The states in a molecular signal transducer are frequently defined by different numbers of phosphorylations of a target protein. Phosphorylation is the covalent attachment of a phosphate group (consumed from an energy-rich ATP molecule), generally at a tyrosine, serine or threonine residue of a protein. Both phosphorylation and dephosphorylation are catalyzed concurrently, by exogenously supplied kinase and phosphatase enzymes. Their rates may also be enhanced by feedback catalysis, wherein the fully phosphorylated product increases the rate of phosphorylation of the remaining partially phosphorylated proteins.

Since the total number of protein molecules involved in these reactions is not large, stochasticity clearly places important limits on the stability of a switch. Thermal fluctuations can jeopardize the reliability or even existence of switches constructed from signaling pathways. Understanding their consequences is hence important, both empirically [8, 9] and theoretically [10, 11, 12, 13].

In this Letter, we construct and analyse a model for a switching circuit, incorporating all the above elements. The model assumes a set of  $N$  proteins that can undergo, independently of each other,  $J$  phosphorylation reactions each. State 0 is fully dephosphorylated and state  $J$  fully phosphorylated. Dephosphorylation also occurs concurrently from each state except 0. The rates of phosphorylation and dephosphorylation are enhanced by feedback from states  $J$  and 0 respectively. We analyse the master equation of this problem, using many-body techniques applied previously to stochastic models of gene expression [14]. The main points of this Letter are threefold. First, the analysis of the model makes clear that the same formalism treats both the emergence

of a bistable phase and its stability as a function of the parameters of the problem. Once bistability is assumed, the scaling of residence times has been bounded quite generally by Bialek [15] for a system described by a single variable. Our model provides a framework within which this might be understood for the more nontrivial case of a multi-variate system. Second, analysis of our model shows that for large  $N$ , bistability occurs for *any*  $J \geq 2$ . This is clearly important in the biochemical context where known  $J$  values range from 1 to 18 [16]. We find, in addition, that the universality class of this phase transition from unistability to bistability, is *different* for finite  $J$  and for infinite  $J$ . We do not know of any other non-equilibrium model which shows this behaviour. Third, we see from the model that the phase transition may be brought about either by keeping the numbers of kinase and phosphatase molecules constant and varying the number of target protein molecules or by keeping the latter fixed and changing the former. When molecular biologists think of control within a fixed circuit architecture, they typically think of varying only the input signal (the kinase and phosphatase molecules, in this case). We see in our system that the number of target molecules also constitutes a degree of freedom for control. In other words a circuit can be switched even when input signals are constant, by changing the expression levels of targets.

A schematic representation of our model is shown in Fig. 1. Phosphorylation states are represented as  $J+1$  lattice sites indexed by  $j \in 0, \dots, J$ , among which the  $N$  protein molecules hop independently forward (by individual phosphorylation) or backward (by dephosphorylation). The forward and backward rates have two components: a part resulting from the externally supplied kinase and phosphatase particles ( $I$  and  $P$  respectively) and a part resulting from feedback catalysis. We have set the strength of the feedback equal to the occupancy of sites 0 (or  $J$ ) for backward (forward) hops, without loss of generality. In all that follows, we analyse the model for the case  $I = P = q$ .

The model incorporates several important abstractions from known biological cases. We have effectively assumed a specific sequence for phosphate attachment, in not assigning combinatorial factors for attachment rates which

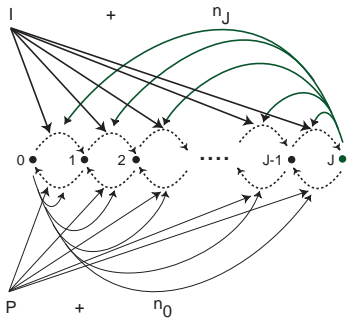


FIG. 1: The symmetrized signal transduction cascade. Number of phosphorylations of the protein define sites  $0 \dots J$ . Dashed arrows represent phosphorylation and dephosphorylation transitions as hopping of a protein among sites, and solid arrows designate catalytic action (thick: phosphorylation, thin: dephosphorylation).  $I$  is the number of externally-supplied kinase particles,  $P$  the number of externally-supplied phosphatase particles, and  $n_J$  and  $n_0$  the number of proteins respectively in the forward and reverse autocatalytic states.

grow at intermediate  $j$ . All catalysts are assumed to act on all transitions, so there is no account of so-called “complex formation”, in which catalysts acting on one particle are unavailable to others. Many signaling cascades employ membrane-bound proteins, and possibly important effects associated with the viscosity or structure of biological membranes are also omitted in the model. More importantly, we assume that the *unphosphorylated* state  $j = 0$  is a catalyst for dephosphorylation, whose rate adds to that of the  $P$  externally-supplied phosphatase particles. It is not known whether any real signal-transduction cascades use such a symmetric autocatalytic scheme, but it greatly simplifies the analysis of large- $N$  behavior of the system in the range relevant to the onset of switching. We also make a simplification in setting  $I = P \equiv q$ . This allows phosphorylation states  $j = 0$  and  $j = J$  to play fully symmetric roles, and renders the two stable states in the bistable phase exactly degenerate.

There are two respects in which nonsymmetric systems, either topologically (where only the  $j = J$  state acts as a catalyst) or through  $I \neq P$ , can differ from the system idealized here. If the topology is symmetric but  $I \neq P$  we expect that one of the two steady states becomes metastable and the transition first-order. If the topology is asymmetric even metastability occurs only at  $I < P$ . But in this case, sufficiently large  $N$  always ensures that the feedback wins and that there is a unique stable state. The biological ramifications of topology and parameter choice will be studied carefully elsewhere [18].

Before presenting details of the analysis, we summarize our results below. The system of Fig. 1 is describable in terms of a single parameter  $g \equiv N/q$ . At small  $g$  values the  $N$  particles are homogeneously distributed over the  $J + 1$  sites of the lattice. In particular, average occupancy  $\langle n_0 \rangle$  of site 0 is equal to the average occupancy

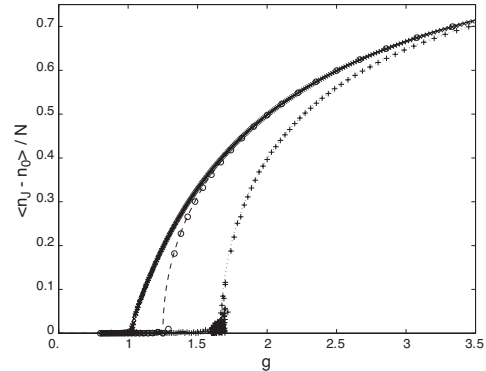


FIG. 2: Order parameter  $|\langle n_J - n_0 \rangle|/N$  for the phosphorylation chain: mean-field theory (lines) and simulations (symbols).  $J + 1 = [5, 10, 100]$  corresponds to [dot, dash, solid] for lines and  $[+, \circ, \times]$  for symbols. Particle numbers used in the simulations are respectively  $N = [4000, 2000, 400]$ .

$\langle n_J \rangle$  of site  $J$ , where the averages are over the steady state distribution. As  $g$  increases, at a value  $g = g_c$ , the system undergoes spontaneous symmetry breaking and the occupancy at either site 0 or  $J$  becomes greater than at the other, until at very large  $g$ , almost all the particles are found at either the fully dephosphorylated state  $j = 0$  or the fully phosphorylated state  $j = J$ . The relevant order parameter describing the system is hence  $|\langle n_J - n_0 \rangle|/N \in [0, 1]$ . Fig. 2 shows our numerical and analytical estimates of this quantity.

The phase transition occurs at any  $J > 1$  at a critical point whose mean-field value is  $g_c = (J + 1)/(J - 1)$ . In a neighborhood of order  $g_c \leq g \lesssim 1 + 2(g_c - 1)$ , the order parameter scales with  $g$  as in Curie-Weiss mean-field ferromagnetism [19], with a  $J$ -dependent normalization:

$$\frac{|\langle n_J - n_0 \rangle|}{N} \approx \frac{\sqrt{6J}}{J + 1} \left( \frac{g}{g_c} - 1 \right)^{1/2}. \quad (1)$$

For  $g \gtrsim 1 + 2(g_c - 1)$  the order parameter saturates to a  $J$ -independent envelope value

$$\frac{|\langle n_J - n_0 \rangle|}{N} \rightarrow 1 - \frac{1}{g}. \quad (2)$$

Since  $g_c - 1 \rightarrow 2/J$  for large  $J$ , Eq. (2) also gives the behavior in the formal  $J \rightarrow \infty$  limit. The derivative of the order parameter converges to one in arbitrarily small neighborhoods of the critical point, rather than to  $\infty$  as in the Curie-Weiss regime; thus  $J \rightarrow \infty$  defines a different universality class than any finite  $J$ , as shown in Fig. 2.

The fluctuations of the order parameter, normalized by the Poisson value  $2N/(J + 1)$ , are dominated by a peak

$$\frac{\langle (n_J - n_0)^2 \rangle - \langle n_J - n_0 \rangle^2}{2N/(J + 1)} \approx \frac{\text{const} \sim 1}{(J + 1)|g - g_c|} \quad (3)$$

The factor  $1/(J + 1)$  arises because a single mode out of  $J + 1$  in the diffusive spectrum goes unstable at the critical point. This mode describes collective fluctuation of

particles between the  $j = 0$  and  $j = J$  limits, and corresponds to the fluctuations in aggregate magnetization in the Curie-Weiss solution. The results for the fluctuation spectrum are shown in Fig. 3.

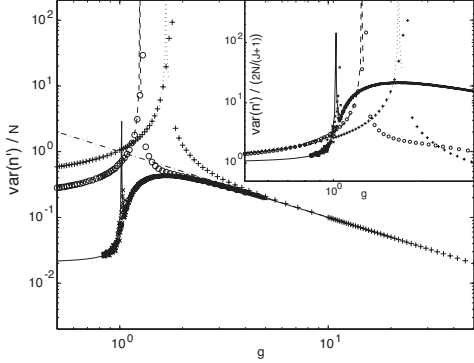


FIG. 3: Fluctuations in the order parameter scaled for  $g$  above and below critical.  $\text{var}(n')$  stands for the variance  $\langle (n_0 - n_J)^2 \rangle - \langle n_0 - n_J \rangle^2$ . Lines are leading-order expansion in fluctuations about the symmetric mean-field solution, continued through  $g_c$ ; symbols from simulation,  $J+1$  values and markers as in Fig. 2. Large panel shows convergence of  $\text{var}(n')$  to  $N/g$  at all  $J$ , and a fit to  $(N/g)(1 - g^{-2.5})$  for  $J+1 = 100$ . Inset shows convergence of  $\text{var}(n')$  to Poisson result  $2N/(J+1)$  as  $g \rightarrow 0$ .

At large  $J$ , the prefactor  $1/(J+1)$  in Eq. (3) reduces the single-mode Curie-Weiss fluctuation peak to zero weight. The  $J \rightarrow \infty$  fluctuation spectrum is hence characterized entirely by renormalized diffusion in an effectively coupled Bose gas. If fluctuations were entirely independent, the mean-field spectrum would be  $\left[ \langle n_0^2 \rangle - \langle n_0 \rangle^2 \right]_{\text{MFT}} = N(1 - 1/g)(1/g)$ . As shown in Fig. 3, however, the large- $J$  background converges to  $\langle n_0^2 \rangle - \langle n_0 \rangle^2 \rightarrow N(1 - 1/g^{2.5})(1/g)$ , indicating that correlated fluctuations dominate.

We now present some details of the analysis of the model. The phosphorylation chain is described instantaneously by a state vector of occupation numbers  $n \equiv (n_0, n_1, \dots, n_J)$ , and the ensemble by a joint probability density  $P(n)$ .  $N \equiv \sum_{j=0}^J \langle n_j \rangle$  is a constant.

The master equation corresponding to the stochastic dynamics of Fig. 1 is

$$\begin{aligned} \frac{d}{dt} P(n) = & \sum_{j=0}^{J-1} [(I + n_J - \delta_{J,j+1})(n_j + 1) P(n + 1_j - 1_{j+1}) \\ & - (I + n_J) n_j P(n) \\ & + (P + n_0 - \delta_{0,j})(n_{j+1} + 1) P(n - 1_j + 1_{j+1}) \\ & - (P + n_0) n_j P(n)], \end{aligned} \quad (4)$$

where  $1_j$  represents the vector of zeros with a 1 in the  $j^{\text{th}}$  position, and  $\delta_{j,j'}$  is the Kronecker delta. Eq. (4) can be

solved perturbatively by introducing an operator algebra on a basis of number states, and so converting  $P(n)$  into an equivalent representation as a state vector. Creation and annihilation operators are introduced [21, 22] with standard commutation relations  $[a_j, a_{j'}^\dagger] \equiv \delta_{j,j'}$ , and a zero-particle state vector  $|0\rangle$  and its conjugate  $\langle 0|$  are defined by the conditions  $a_j|0\rangle \equiv 0, \forall j$ ,  $\langle 0|a_j^\dagger \equiv 0, \forall j$ . Number states are defined as

$$|n\rangle \equiv \prod_{j=0}^J \left( a_j^\dagger \right)^{n_j} |0\rangle, \quad (5)$$

and normalized as [22]  $\langle 0| \exp \left( \sum_j a_j \right) |n\rangle = 1, \forall n$ . The  $j^{\text{th}}$  number operator has the usual representation  $\hat{n}_j \equiv a_j^\dagger a_j$ , and  $\langle 0| \exp \left( \sum_{j'} a_{j'} \right) \hat{n}_j |n\rangle = n_j$ .

The master equation (4) has the corresponding representation

$$\frac{d}{dt} |\psi\rangle = -\Omega |\psi\rangle, \quad (6)$$

with  $|\psi\rangle \equiv \sum_n P(n) |n\rangle$ , and the evolution operator

$$\Omega = q \sum_{j=0}^{J-1} \left( a_{j+1}^\dagger - a_j^\dagger \right) \left[ \left( 1 + \frac{\hat{n}_0}{q} \right) a_{j+1} - \left( 1 + \frac{\hat{n}_J}{q} \right) a_j \right]. \quad (7)$$

The integral of Eq. (6),  $|\psi_t\rangle \equiv e^{-\Omega t} |\psi_0\rangle$ , is converted to a functional integral by the insertion of the coherent-state representation of the identity operator

$$\int \frac{d\phi_{t'}^\dagger d\phi_{t'}}{\pi} e^{-\phi_{t'}^\dagger \cdot \phi_{t'}} e^{a^\dagger \cdot \phi_{t'}} |0\rangle \langle 0| e^{\phi_{t'}^\dagger \cdot a} = \sum_n |n\rangle \langle n| = I \quad (8)$$

at a set of times  $t' = k\Delta t \in (0, t)$ .  $\phi_t$  is a column vector of  $J+1$  complex coefficients, and  $\phi_t^\dagger$  its adjoint. If we take as a convenient choice of initial state  $|\psi_0\rangle = \exp \left( \sum_j \bar{n}_j (a_j^\dagger - 1) \right) |0\rangle$ , we obtain by standard methods [22] the relation for the normalized partition function

$$\langle 0| \exp \left( \sum_j a_j \right) |\psi_t\rangle = \int \mathcal{D}\tilde{\phi} \mathcal{D}\phi e^{-\int dt L} e^{\tilde{\phi}_0 \cdot (\bar{n} - \phi_0)}, \quad (9)$$

in which the diffusion-“Lagrangian” is

$$L(\tilde{\phi}, \phi) = \tilde{\phi} \cdot \frac{\partial \phi}{\partial t} + \Omega(\tilde{\phi} + 1, \phi). \quad (10)$$

The field  $\phi_t^\dagger$  is shifted in notation as  $\phi_t^\dagger \equiv \tilde{\phi}_t + 1$ , to cancel the surface term from the normalization, and the function  $\Omega(\tilde{\phi} + 1, \phi)$  in Eq. (10) has the form of Eq. (7), with the substitutions  $a_j^\dagger \rightarrow \tilde{\phi}_j + 1$ ,  $a_j \rightarrow \phi_j$ .

The mean number density is related to the integration variables as  $\langle \phi_{j,t} \rangle = \langle n_{j,t} \rangle$ , where the first  $\langle \rangle$  denotes average in the functional integral (9), and the second the equivalent average under  $P(n)$ . The mean-field

solution for the order parameter is obtained from the stationary-point approximation of  $\langle \phi_{jt} \rangle$  by the solution  $\bar{\phi}$  to  $\partial L / \partial \tilde{\phi} \Big|_{\tilde{\phi} \equiv 0} = 0$ , and recovers Eq. (1) and Eq. (2) in appropriate limits. Fluctuations are computed by shifting the integration variables  $\tilde{\phi} \equiv 0 + \tilde{\phi}'$ ,  $\phi \equiv \bar{\phi} + \phi'$ , and expanding  $L$  to second order in primes, to obtain a matrix equation of the form

$$L = \tilde{\phi}' D_0 \phi' + \tilde{\phi}' D_2 \tilde{\phi}'^T. \quad (11)$$

$D_0$  is the diffusion operator in the stationary background, and  $D_2$  is a kernel whose eigenvalues govern the Gaussian noise spectrum of the stochastic process.

Manipulation of the operators in the functional integral gives the corresponding fluctuation relation, used in Fig. 3:

$$\frac{\langle (n_J - n_0)^2 \rangle - \langle n_J - n_0 \rangle^2}{2N/(J+1)} = 1 + \frac{J+1}{N} \left\langle \left( \frac{\phi'_J - \phi'_0}{\sqrt{2}} \right)_t^2 \right\rangle. \quad (12)$$

The important property of the matrix  $D_2$  in Eq. (11) is that it has a single negative eigenvalue at all  $g$ , whose fluctuations may be removed in exchange for a Langevin field, which then drives the noise spectrum of the ensemble, just as in classical reaction-diffusion [22]. All other eigenvalues of  $D_2$  are zero in the symmetric phase, and a single positive eigenvalue appears in the symmetry-broken phase.

Also from Eq. (11), the Green's function which propagates the Langevin fluctuations may be expanded in

eigenvectors of  $D_0$ . Elementary algebra shows that only the lowest antisymmetric eigenvector becomes degenerate at the critical point, leading to the Curie-Weiss divergence with weight  $1/(J+1)$  of Eq. (3). The remainder of the eigenvectors remain close to ordinary diffusive solutions in the symmetric phase, leading to the regular component of the fluctuation spectrum in Fig. 3. These details, as well as an analysis of the symmetry-broken phase, will be provided in a longer paper [23].

To conclude: in attempting to understand as a many-body effect the stability of a signal-transduction element based on multiple phosphorylation with feedback, we have found that the onset of bistability is a second-order phase transition at large  $N$ . Qualitatively the distinction between small- $J$  and large- $J$  behavior at this transition is determined by whether one or both reflecting boundaries are sensed by the near-critical symmetry-broken state. For small  $J$  all sites remain macroscopically occupied close to the transition point. For large  $J$ , only a finite number of sites dependent on  $g$  but not on  $J$  are populated.

The most important feature of the model that still remains to be investigated is the residence time within states in the symmetry-broken phase as a function of  $N$  and  $g$ . This feature is of biological interest, since it pertains to the memory of switches at finite temperature. For a system described by a single occupation variable, this has been bounded above by an exponential in  $N$  [15]. For a multi-variate system, this bound should only receive polynomial corrections. However this remains to be computed.

---

[1] B. Novak, Z. Pataki, A. Ciliberto, and J. J. Tyson, *Chaos* **11**, 277 (2001).  
[2] J. J. Tyson, A. Csikasz-Nagy, and B. Novak, *Bioessays* **24**, 1095 (2002).  
[3] J. E. Ferrell, Jr., *Bioessays* **21**, 833 (1999).  
[4] J. E. Ferrell and W. Xiong, *Chaos* **11**, 227 (2001).  
[5] J. E. Lisman, *Proc. Natl. Acad. Sci. USA* **82**, 3055 (1985).  
[6] C. Y. Huang and J. E. Ferrell, Jr., *Proc. Natl. Acad. Sci. USA* **93**, 10078 (1996).  
[7] J. J. Tyson, K. C. Chen, and B. Novak, *Curr. Opin. Cell Biol.* **15**, 221 (2003).  
[8] M. B. Elowitz, A. J. Levine, E. D. Siggia, and P. S. Swain, *Science* **297**, 1183 (2002).  
[9] E. M. Ozbudak, M. Thattai, I. Kurtser, A. D. Grossman, and A. Oudenaarden, *Nat. Genet.* **31**, 69 (2002).  
[10] H. H. McAdams and A. Arkin, *Trends Genet.* **15**, 65 (1999).  
[11] J. Paulsson and M. Ehrenberg, *Q. Rev. Biophys.* **34**, 1 (2001).  
[12] M. Thattai and A. Oudenaarden, *Proc. Natl. Acad. Sci. USA* **98**, 8614 (2001).  
[13] C. V. Rao, D. M. Wolf, and A. P. Arkin, *Nature* **420**, 231 (2002).  
[14] M. Sasai and P. Wolynes, *Proc. Natl. Acad. Sci. USA* **100**, 2374 (2003).  
[15] W. Bialek, in *Advances in Neural Information Processing*, Vol. 13, T. K. Leen, T. G. Dietterich, and V. Tresp, eds., (MIT Press, Cambridge, 2001)  
[16] We obtained this range from an analysis of the Phospho-base, a database of experimentally certified phosphorylatable proteins [17].  
[17] A. Kreigipuu, N. Blom, and S. Brunak, *Nucleic Acids Res.* **27**, 237 (1999).  
[18] W. Fontana, D. Krakauer, S. Krishnamurthy, and E. Smith, “Stochastic Molecular Switches”, in preparation.  
[19] N. Goldenfeld, *Lectures on Phase Transitions and the Renormalization Group*, Frontiers in Physics Series, Addison-Wesley (1992).  
[20] G. L. Eyink, *Phys. Rev. E* **54**, 3419 (1996).  
[21] D. C. Mattis and M. L. Glasser, *Rev. Mod. Phys.* **70**, 979 (1998).  
[22] J. L. Cardy, lectures presented at the Troisième Cycle de la Suisse Romande, Spring 1999, ([www-thphys.physics.ox.ac.uk/users/JohnCardy/](http://www-thphys.physics.ox.ac.uk/users/JohnCardy/))  
[23] E. Smith, S. Krishnamurthy, D. Krakauer, and W. Fontana, “The statistical mechanics of biomolecular switching”, in preparation.